Portugaliae Electrochimica Acta 2014, 32(5), 355-367

DOI: 10.4152/pea.201405355

PORTUGALIAE ELECTROCHIMICA ACTA
ISSN 1647-1571

Evaluation of Corrosion Inhibition of Mild Steel: Chemically Polymerized PpAP/ Al_2O_3 Composite in the Presence of Anionic Surfactants

G. Thenmozhi,[a] P. Arockiasamy,[a] G. Mohanraj,[b] Jaya Santhi R[a,*]

[a] *P G & Research Department of Chemistry, Auxilium College, Vellore-632006, Tamil Nadu, India*
[b]*Department of Physics, Martin Luther University of Halle-wittenberg, Halle(saale)-06120, Germany*

Received 15 October 2014; accepted 25 October 2014

Abstract

Poly para aminophenol (PpAP)/Al_2O_3 composite was prepared by *in situ* chemical polymerization of para aminophenol using ammonium persulphate as an oxidizing agent in an aqueous medium containing anionic surfactants like DBSA (dodecyl benzene sulphonic acid) and SDS (sodium dodecyl sulphate) at 0 ˚C. The synthesized composites were characterized by UV–VIS-NIR spectroscopy, FTIR, XRD and TGA. The inhibiting effect of synthesized composites on the corrosion of mild steel in 1 M HCl solution has been investigated by different techniques like potentiodynamic polarization and electrochemical impedance spectroscopy methods for four different concentrations ranging from 50 to 300 mg/L. The results indicated that the corrosion inhibition efficiency increased on increasing composites concentration till 200 mg/L and decreased on further increasing concentration. It has been found that PpAP/Al_2O_3-DBSA has got higher corrosion protection efficiency than that of PpAP/ Al_2O_3-SDS. Polarization studies reveal that composites act as a mixed type corrosion inhibitor and adsorption follows Langmuir adsorption isotherm.

Keywords*:* aminophenol, oxidative polymerization, surfactant, corrosion protection, mild steel.

Introduction

The damage by corrosion generates not only high cost for inspection, repairing, and replacement, but in addition it constitutes a public risk, thus the necessity of

* Corresponding author. E-mail address: shanthijaya02@gmail.com

developing novel substances that behave like corrosion inhibitors especially in acid media [1]. The use of inhibitors is one of the most effective and often successful methods of protection of corrosion of metals in acidic media. It is a well-known fact that acids are used in many operations such as pickling, cleaning, descaling, etc. Because of their aggressiveness, inhibitors are used to reduce the rate of dissolution of metals [2]. Among the acid solutions, hydrochloric acid is one of the most widely used in the pickling processes of metals. The use of organic molecules as corrosion inhibitors is one of the most practical methods for protecting against corrosion, and it is becoming increasingly popular. It has been shown that organic compounds containing heteroatoms with high electron density, such as phosphorus, nitrogen, sulfur, and oxygen, as well as those containing multiple bonds which are considered as adsorption centers, are effective as corrosion inhibitors [3-6].

A derivative of polyaniline, aminophenols are interesting electrochemical materials since, unlike aniline and other substituted anilines, they have two groups ($–NH_2$ and –OH) which can be oxidized [7]. Recently, poly aminophenol has attracted considerable attention for the preparation of its composites with inorganic particles in the presence of surfactants to improve their process ability. Surfactant inhibitors have many advantages, for example, high inhibition efficiency, low price, low toxicity, and easy production. Moreover, the investigation of surfactants adsorbed on metal surfaces is extremely important in electrochemical studies such as corrosion inhibition, adhesion, lubrication, and detergency [8]. The most important action of inhibition is the adsorption of the surfactant functional group onto the metal surface, as adsorption is critical to corrosion inhibition. The ability of a surfactant molecule to adsorb is generally related to its ability to aggregate to form micelles. Zhao and Mu [9] observed the effect of anionic surfactants such as dodecyl sulphonic acid sodium salt (DSASS), dodecyl benzene sulfonic acid sodium salt (DBSASS) and SDS on aluminium surfaces.

In the present work, PpAP/Al_2O_3 composite was prepared in the presence of two anionic surfactants like DBSA and SDS by chemical oxidation method and characterized by different spectroscopic techniques. An attempt has been made to investigate the corrosion protection behaviour of chemically synthesized PpAP/Al_2O_3-DBSA and PpAP/Al_2O_3-SDS composites over mild steel (MS) in acidic environment using potentiodynamic polarization and electrochemical impedance spectroscopy (EIS) measurements.

Experimental method

Synthesis of PpAP/Al_2O_3 composites

The equimolar volumes of 0.1 M solution of para aminophenol and HCl were prepared in double distilled water, mixed and kept in the freezing mixture. 2 g of Al_2O_3 were added to the above solution and kept for vigorous stirring to keep the Al_2O_3 suspended in the solution. 0.1 M ammonium per sulphate and 0.025 M DBSA were taken in separate beakers. The oxidant and surfactant were added slowly to the mixture containing para aminophenol and Al_2O_3 and the stirring

was continued for six hours at 0 ˚C. The product was filtered, washed with excess amount of water, methanol and acetone to remove excess of HCl, APS and DBSA. The resulting composite was then dried at 50 ˚C for 24 h. The same procedure was adopted for the synthesis of PpAP- Al_2O_3 /SDS composite.

Characterization

UV-VIS-NIR spectra of composites dissolved in DMSO solvent were obtained using a Varian, Cary-5000 spectrophotometer in the range of 200-2500 nm. The FT-IR spectra were recorded by a Thermo Nicolet, Avatar 370 spectrophotometer. The spectrum of the dry polymer powder in KBr pellet was recorded from 500 cm^{-1} to 4000 cm^{-1}. X-ray diffraction (XRD) scan was done with a Bruker AXS D8 Advance diffractometer at room temperature using Cu Kα (λ=1.5406 A˚). Thermo gravimetric analysis (TGA) was carried out in nitrogen atmosphere at a heating rate 10 ˚C/min up to 750 ˚C temperature by a Perkin Elmer, Diamond TG/DTA analyzer.

Preparation of specimens

Mild steel specimens having nominal composition of 0.023% P; 0.04% Si; 0.017% Ni; 0.37% Mn; 0.078% C; 0.02% S; 0.002% Mo and Fe balance were used. Specimen of dimension 1 × 1× 0.1 cm was used for electrochemical studies. The specimens were embedded in epoxy resin leaving a working area of 1 cm^2. The surface preparation of the mechanically abraded specimens was carried out using different grades of silicon carbide emery paper (up to 1200 grit) and subsequent cleaning with acetone and rinsing with double-distilled water were done before each experiment.

Electrolyte

An electrolyte of 1 M HCl solution was prepared by diluting 37% HCl (Merck) using double-distilled water, being used as a corrosive solution. The four concentrations of PpAP/Al_2O_3 composites varying from 50 to 300 mg/L were used for the present investigations.

Electrochemical measurements

Electrochemical measurements, including potentiodynamic polarization curves and EIS were performed in a conventional three electrode cell using a computer-controlled potentiostat/galvanostat (Autolab PGSTAT 302N potentiosat from Eco-chemie, Netherlands). A platinum electrode was used as the counter electrode, Ag/AgCl, 3 M KCl as the reference electrode, and the mild steel specimen was used as a working electrode. Before each potentiodynamic polarization (Tafel) and EIS studies, the electrode was allowed to corrode freely and its open circuit potential (OCP) was recorded as a function of time up to 20 min, which was sufficient to attain a stable state. After this, a steady-state of OCP corresponding to the corrosion potential (E_{corr}) of the working electrode, was obtained. The potentiodynamic measurements were started from cathodic to the anodic direction, E = E_{corr} ± 250 mV, at a scan rate of 10 mVs^{-1}. The linear Tafel segments of the anodic and cathodic curves were extrapolated to obtain E_{corr} and

the corrosion current density (I_{corr}). The inhibition efficiency was evaluated from the measured I_{corr} with and without inhibitor using the relationship,

$$IE(\%) = \frac{I^0_{corr} - I_{corr}}{I^0_{corr}} \times 100 \quad (1)$$

where I^0_{corr} is the corrosion current density without inhibitor, and I_{corr} is the corrosion current density with inhibitor. The corrosion rates of MS with polymers were calculated from polarization curves using the following equation [10],

$$CR = \frac{3.27 \times 10^{-3} I_{corr} (EW)}{D} \quad (2)$$

where CR is the corrosion rate (mmpy), I_{corr} is the corrosion current density (μA cm^{-2}), EW is the equivalent weight of the specimen, and D is the density (g cm^{-3}) of the specimen.

EIS measurements were carried out using AC signals of 10 mV for the frequency spectrum from 100 kHz to 10 mHz at the stable OCP. The potentiodynamic polarization and EIS data were analyzed and fitted using graphing and analyzing impedance software, Nova 1.4. Fresh solution and fresh steel samples were used after each sweep. The charge transfer resistance (R_{ct}) was obtained from the diameter of the semicircle of the Nyquist plot. The inhibition efficiency of the inhibitor has been found out from the charge transfer resistance values using the following equation

$$IE(\%) = \frac{R_{ct} - R^0_{ct}}{R_{ct}} \times 100 \quad (3)$$

where R^0_{ct} and R_{ct} are the charge transfer resistance in the absence and in the presence of the inhibitor, respectively.

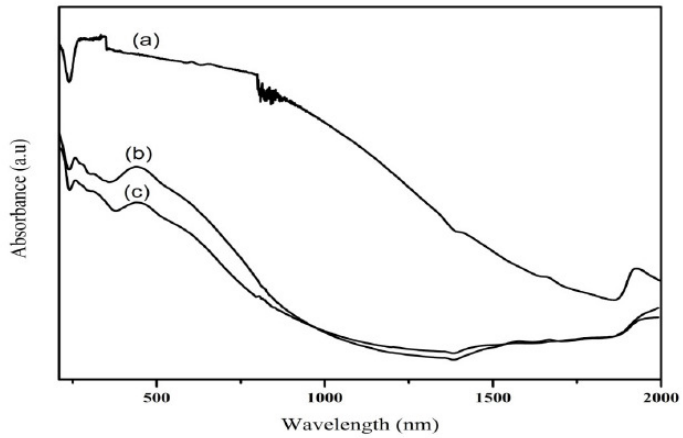

Figure 1. UV-VIS-NIR spectra of (a) PpAP, (b) PpAP/Al_2O_3-SDS and (c) PpAP/Al_2O_3 –DBSA.

Results and discussion

UV-VIS-NIR spectroscopy

The UV/VIS/NIR absorption spectra of PpAP and PpAP/Al_2O_3 composites dissolved in DMSO are shown in Fig. 1, where we clearly observe two

characteristic absorption peaks of PpAP: the first peak at 252-265 nm is assigned to the $\pi - \pi^*$ transition of the phenyl rings which is related to the extent of conjugation between the phenyl rings in the polymer chain; the second absorption peak at 425–440 nm shows n-π^* transitions within the quinoid structure [11]. In addition, from comparison of UV–VIS-NIR spectra PpAP/ Al_2O_3-DBSA and PpAP/Al_2O_3- SDS can be seen that the shapes of peaks were very similar, but there are some shifts due to the interaction between PpAP/ Al_2O_3 and surfactants. It is well known that in composites systems with PpAP, strong guest–host interactions, such as hydrogen bonding, occur in the form of NH· · ·O -Al in Al_2O_3 [12].

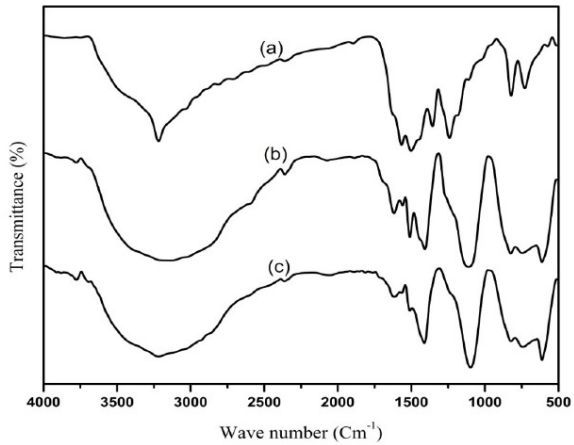

Figure 2. FT-IR spectra of (a) PpAP, (b) PpAP/Al_2O_3-DBSA and (c) PpAP/Al_2O_3 – SDS.

FT-IR analysis

Fig. 2 shows the FTIR spectra of PpAP and PpAP/Al_2O_3 composites synthesized in two different surfactants. The main characteristic peaks of PpAP are assigned as follows: the broad intense peak around 3219 cm^{-1} is assigned to O–H stretching vibrations; a shoulder peak at 1504 cm^{-1} is due to stretching vibrations of N–H in the secondary amine, indicating that the polymerizing chains grow through the amino groups; the two main peaks around 1600 and 1560 cm^{-1} correspond, respectively, to the ring-stretching vibrations of the quinoid and benzenoid rings [13]; the peak at 1364 cm^{-1} is due to C - N stretching vibration of a secondary aromatic amine; the peak at 1121 cm^{-1} is ascribed to the stretching vibration of C- O- C linkages and further support that the P-aminophenol changed into PpAP [14]. From the FTIR spectra of PpAP/Al_2O_3 composites, it is shown that all the characteristic peaks of PpAP are present and these peaks, when compared to that of PpAP/Al_2O_3, are found to be shifted slightly. It can be concluded that there is an interaction between PpAP macromolecule and Al_2O_3 particles. The interaction may be associated with the interaction of aluminium and nitrogen atoms in PpAP macromolecule. Moreover, the action of hydrogen bonding between Al_2O_3 particles and PpAP molecule is also contributory to the shift of peaks.

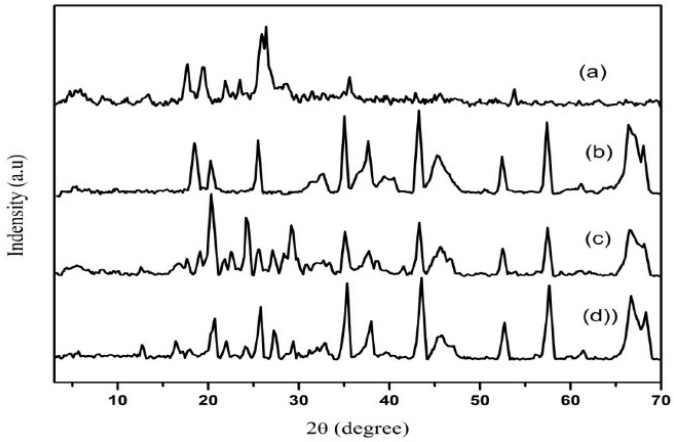

Figure 3. XRD patterns of (a) PpAP, (b) Al_2O_3, (c) PpAP/Al_2O_3–SDS and (d) PpAP/Al_2O_3 –DBSA.

XRD analysis

Fig. 3 shows the XRD pattern of TiO_2, PpAP and PpAP/Al_2O_3 composites. The crystalline regions in PpAP are shown by the presence of relatively sharp peaks. The amorphous regions are visible by the broad low intense peaks. PpAP exhibits broad Bragg diffraction peaks at 2θ angles of 17.6˚, 19.4˚, 24.2˚ and 25.5˚; 2Θ= 25.5˚ is characteristic of the van der Waals distances between stacks of phenylene rings (poly aminophenol rings). These strongest peaks indicate crystalline domains in the amorphous structure of the polymers [15]. It can be seen that the XRD patterns of PpAP/Al_2O_3-DBSA and PpAP-Al_2O_3/SDS are very much similar to that of Al_2O_3 and the broad diffractive peak of PpAP has become weak. The result suggests that the addition of Al_2O_3 hampers the crystallization of the PpAP molecular chain. This is because when the deposited PpAP is absorbed on the surface of the Al_2O_3 particle, the molecular chain of absorbed PpAP is tethered, and the degree of crystallinity decreases. It also confirms that the PpAP deposited on the surface of Al_2O_3 has no effect on the crystalline structure of Al_2O_3.

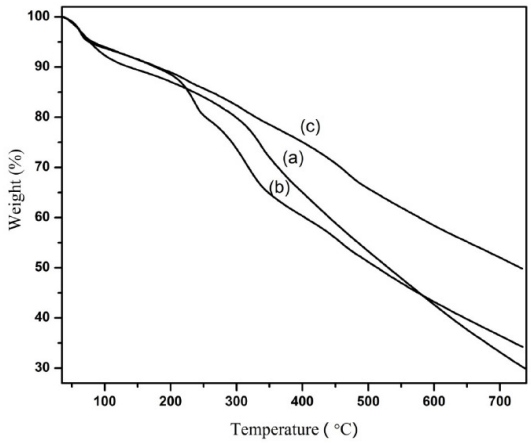

Figure 4. TGA curves of (a) PpAP, (b) PpAP/Al_2O_3-SDS and (c) PpAP/Al_2O_3 –DBSA.

Thermo Gravimetric analysis

The most significant and consistent study of heat stable polymer and composite is the estimation of thermal stability. Thermal properties and interactions between polymer molecule and composite can also be studied from the decomposition through TGA. TGA thermogram (Fig. 4) of PpAP and PpAP/Al_2O_3 composites undergoes three weight loss steps. The first weight loss occurring around 65 ˚C is due to the loss of water vapor from both the oxide and polymer surface. The second weight loss stage which occurs in the range 230 to 310 ˚C corresponds to the removal of HCl, sublimation and removal of low molecular weight polymer/oligomer from the polymer matrix. The third weight loss, around 330 to 455 ˚C, is due to decomposition of the polymer backbone in PpAP, removal of DBSA from PpAP/Al_2O_3-DBSA and SDS dopant from PpAP/Al_2O_3-SDS in composites. The decomposition of PpAP is continuous up to 700 ^oC and even after 700 ^oC the complete decomposition had not take place. The decomposition of PpAP and PpAP/Al_2O_3 composites leaves some char content.

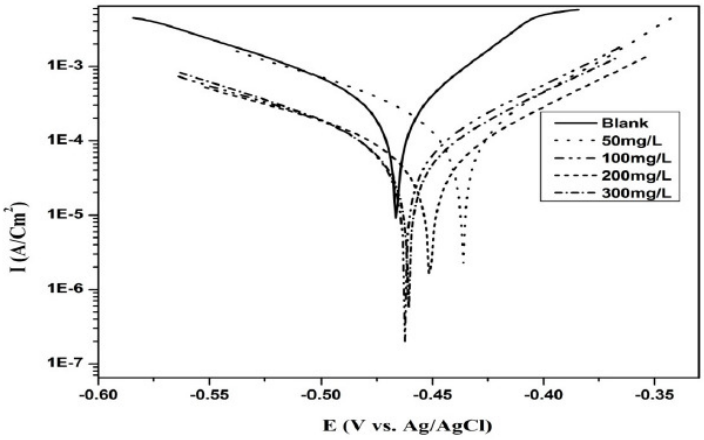

Figure 5a. Potentiodynamic polarization curves obtained for mild steel in 1 M HCl in the presence and absence of different concentrations of PpAP/Al_2O_3 –DBSA.

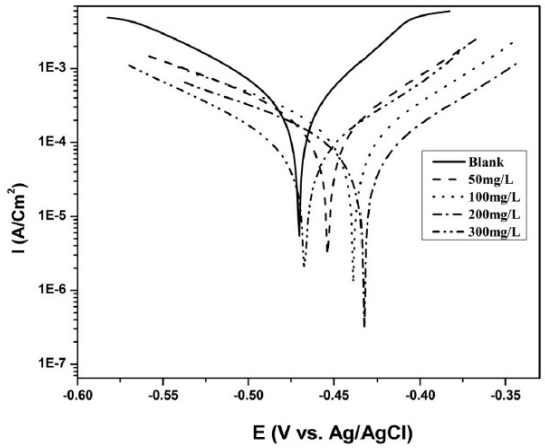

Figure 5b. Potentiodynamic polarization curves obtained for mild steel in 1 M HCl in the presence and absence of different concentrations of PpAP/Al_2O_3 –SDS.

From the TGA curve it can be seen that the degradation of PpAP/Al_2O_3 composites is somewhat similar to that of PpAP. The noticeable difference is that

the thermal decomposition of the composites starts at much lower temperature than that in pure PpAP, which may be due to the strong interaction between PpAP and Al_2O_3 [16]. This is also clear from the XRD where sharp peak of PpAP disappeared in the composites probably due to the interaction of PpAP and Al_2O_3. Several reports show that the lowered thermal stability of polymer composites with the incorporation of inorganic materials is due to the weakened interfacial interaction between the two components [17-18].

Potentiodynamic polarization

The potentiodynamic anodic and cathodic polarization plots for MS specimens in 1 M HCl solution with the synthesized PpAP/Al_2O_3 composites at four different concentrations like 50, 100, 200 and 300 mg/L are given in Fig. 5 and their respective electrochemical parameters, such as corrosion current density (I_{corr}), corrosion potential (E_{corr}), cathodic Tafel slope (b_c), anodic Tafel slope (b_a), inhibition efficiency (IE), degree of surface coverage (θ) and corrosion rate (CR) are given in Table 1. From the values given in this table it is evident that as the inhibitor concentration increased, the corrosion current densities of MS decreased till 200 mg/L of PpAP/Al_2O_3 composites and this behaviour is due to the adsorption of the inhibitor on MS/solution interfaces. The I_{corr} values decrease from 2830 μAcm^{-2} to 72 and 81 μAcm^{-2} with the addition of 200 mg/L of PpAP/Al_2O_3-DBSA and PpAP/Al_2O_3-SDS which resulted in 97.4 and 97.1% of IE. It is clear that the I_{corr} values decrease with the presence of composites, which indicated that composites adsorbed on the metal surface and hence inhibition occurs. Both the composites reached optimum inhibition concentration at 200 mg/L and further increase in concentration the IE value decreases. The E_{corr}, b_a and b_c values do not change appreciably with the addition of the inhibitors, indicating that the inhibitors are not interfering with the anodic dissolution or cathodic hydrogen evolution reactions independently, but they act as a mixed type of inhibitor [19]. These results confirm that the composites on MS act as a highly protective layer, which is mainly attributed to the presence of π electrons in aromatic ring coexisting with quaternary nitrogen atom and large molecular size [7]. The surface coverage is approximately 0.960 (PpAP/Al_2O_3-DBSA) and 0.955 (PpAP/Al_2O_3-SDS) which is good to act as corrosive inhibitors.

Electrochemical impedance spectroscopy

Nyquist plots of MS in 1 M HCl solution in the absence and presence of PpAP /Al_2O_3 composites at different concentrations as inhibitor during an immersion time of 20 min at room temperature are given in Fig. 6.

The depression in the figure is the characteristic of the inhomogeneities of the metal surface during corrosion [20]. The diameter of the capacitive loop stands for the resistance of the corrosion and it can be seen that the resistance decreases significantly with the decrease in diameter. Considering the impedance diagrams, the size of the capacitive loop increased by increasing the concentration of the inhibitor. The Nyquist impedance plots were analyzed by fitting the experimental data to a simple equivalent circuit model given in Fig. 7.

Table 1. Potentiodynamic polarization parameters for mild steel without and with different concentrations of PpAP/Al_2O_3 composites in 1 M HCl.

Inhibitor concentration (mg/L)	b_a (mV/decade)	b_c (mV/decade)	E_{corr} (mV)	I_{corr} (μA/cm^2)	IE (%)	Θ	CR (mm/Year)
PpAP/ Al_2O_3-DBSA							
Blank	44	74	466	2830	-	-	16.23
50	81	49	464	173	93.9	0.94	2.01
100	82	58	462	110	96.1	0.96	1.28
200	86	57	451	72	97.4	0.97	0.84
300	81	59	460	88	96.8	0.97	1.02
PpAP/ Al_2O_3-SDS							
Blank	44	74	466	2830	-	-	16.23
50	107	75	453	196	93	0.93	2.27
100	115	84	438	149	94.7	0.95	1.73
200	123	83	433	81	97.1	0.97	0.95
300	82	69	467	93	96.7	0.97	1.08

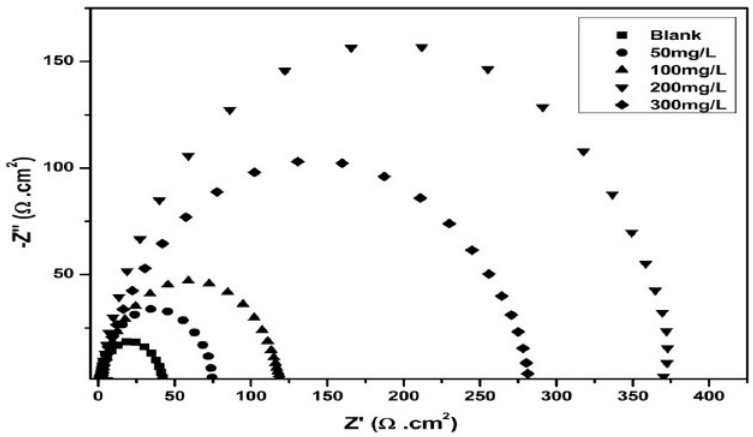

Figure 6a. Nyquist plots obtained for mild steel in 1 M HCl in the presence and absence of different concentrations of PpAP/Al_2O_3 –DBSA.

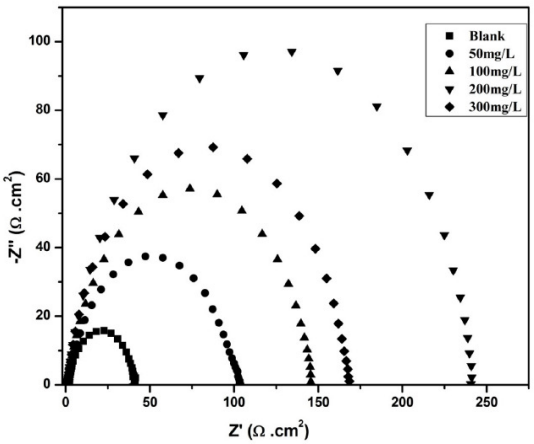

Figure 6b. Nyquist plots obtained for mild steel in 1 M HCl in the presence and absence of different concentrations of PpAP/Al_2O_3 –SDS.

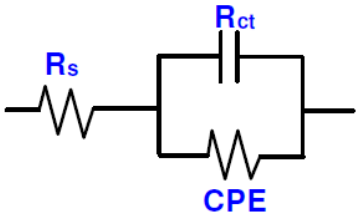

Figure 7. Equivalent circuit model used to fit the metal/solution interface.

In this equivalent circuit (Fig. 7), R_s is the solution resistance, R_{ct} is the charge transfer resistance, and CPE is a constant phase element, which is placed in parallel to charge transfer resistance element. Thus, in these situations, pure double layer capacitors are better described by a transfer function with constant phase elements (CPE) to give a more accurate fit [21] and its impedance is given by

$$Z = A^{-1} (i\omega)^{-n} \qquad (4)$$

where A is the proportionality coefficient, ω is the angular frequency, i is an imaginary number, and n is an exponent related to the phase shift and can be used as a measure of the surface irregularity. For ideal electrodes, when $n = 1$, CPE can be considered as a real capacitor. The R_{ct} values are calculated based on the difference in impedance at lower and higher frequencies. According to Helmholtz, the decrease in CPE can be attributed to increase in the thickness of the electrical double layer [22]. The electrochemical parameters derived from Nyquist plots are calculated and listed in Table 2, indicating that the values of both R_{ct} and IE are found to increase with increasing the inhibitor concentration, while the values of double layer capacitance (C_{dl}) are found to decrease. The R_{ct} value is increased from 39.79 Ω cm^2 for blank solution to 374.86 and 240.77 Ω cm^2 upon addition of 200 mg/L of PpAP/Al_2O_3-DBSA and PpAP/Al_2O_3-SDS, resulting in 89.39 and 83.47% IE, respectively. The increase in R_{ct} value is attributed to the formation of an insulating protective film at the metal/solution interface [23]. The C_{dl} decreases from 8.32μF cm^{-2} to 1.28 and 4.89 μF cm^{-2} in the presence of 200 mg/L of PpAP/Al_2O_3-DBSA and PpAP/Al_2O_3-SDS, respectively. The effect is reversed with further increase in the concentration of the composites as seen in the result. As the concentration of the composites increased above 200 mg/L, the corrosion resistance decreased. In fact, the highest IE was reached at 200 mg/L of both the composites, which is considered as being an optimum inhibitor concentration. The initial decrease in C_{dl} value from blank solution to that of the inhibitor containing electrolyte is due to a decrease in the local dielectric constant, while further decrease in C_{dl} with increasing concentrations of the inhibitor is due to increase in the thickness of the electrical double layer. The Θ is approximately 0.742 (PpAP/Al_2O_3-DBSA) and 0.733 (PpAP/Al_2O_3-SDS) which is found to be good to act as an anticorrosive agent. The results obtained from EIS method are in good agreement with the linear polarization measurement.

The enhanced corrosion protection of MS by PpAP/Al_2O_3 composites can be explained on the basis of the molecular adsorption. The composites inhibit

corrosion by controlling both the anodic and cathodic reactions. In acidic solution, the composite molecules exist as protonated species [24]. These protonated species adsorb on the cathodic sites of MS and decrease the evolution of hydrogen. The adsorption on anodic sites occurs through long π-electrons of aromatic rings (benzenoid and quinoid) and lone pair of electrons of nitrogen atoms, which decrease the anodic dissolution of MS [25]. It is well known that the species having high molecular weight and bulky structure may cover more area on the active electrode surfaces. The slightly higher performance of the PpAP/ Al_2O_3-DBSA than PpAP/ Al_2O_3-SDS is due to the higher molecular size and high electron density on the adsorption centers.

Table 2. Impedance parameters for mild steel in 1 M HCl in the presence and absence of different concentrations of PpAP/Al_2O_3 composites.

Inhibitor concentration (mg/L)	C_{dl} (μF/cm^2)	R_{ct} (Ω Cm^2)	IE (%)	Θ
		PPAP/Al_2O_3-DBSA		
Blank	8.32	39.79	-	
50	7.21	84	52.63	0.526
100	6.86	127.24	68.73	0.687
200	1.28	374.86	89.39	0.894
300	2.45	282.07	85.89	0.859
		PPAP/Al_2O_3-SDS		
Blank	8.32	39.79	-	-
50	7.82	102.2	61	0.61
100	6.90	144.63	72.48	0.725
200	4.89	240.77	83.47	0.835
300	6.52	167.1	76.19	0.762

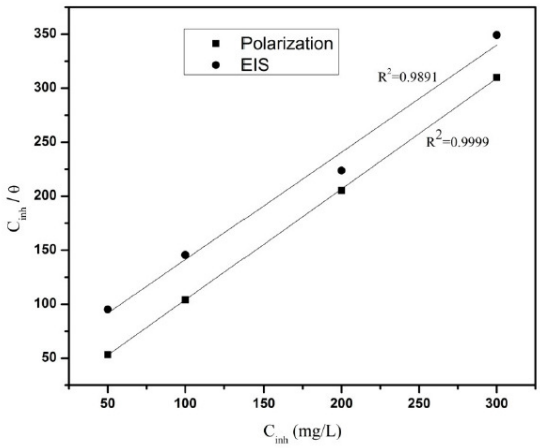

Figure 8. Langmuir adsorption isotherm for MS in 1 M HCl solution of PpAP/Al_2O_3 - DBSA composite at different concentrations.

Adsorption isotherm

The interaction between an inhibitor and MS surface can be described by the adsorption isotherm. We have obtained the adsorption isotherm through the degree of surface coverage which is defined as θ=IE%/100. It was determined at

different inhibitor concentrations using Langmuir adsorption isotherm and can be expressed as

$$C_{inh}/\theta = 1/K + C_{inh} \quad (5)$$

where K is the equilibrium constant of adsorption and C_{inh} is the inhibition concentration. Many researchers have explained the Langmuir adsorption isotherm with the interaction of adsorbed species on the metallic surfaces [26]. The Langmuir adsorption isotherm was drawn by plotting C_{inh}/θ vs. C_{inh}, considering the θ values from potentiodynamic polarization and EIS measurements at 25 ˚C for MS in 1 M HCl at different concentrations of composites; the graph is shown in Fig. 8 and 9. The straight line obtained in the graphs clearly shows that the chosen inhibitor obeys the Langmuir adsorption isotherm. From this, it can be concluded that the PpAP /Al_2O_3 composites can act as a good inhibitor.

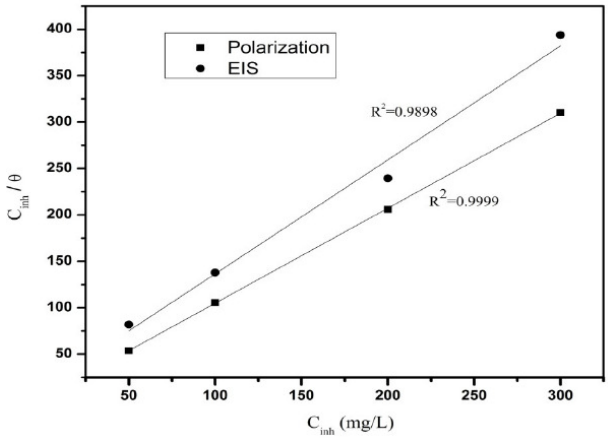

Figure 9. Langmuir adsorption isotherm for MS in 1 M HCl solution of PpAP/Al_2O_3 - SDS composite at different concentrations.

Conclusion

PpAP/Al_2O_3 composites were successfully synthesized by *in situ* chemical oxidative polymerization method using ammonium per sulphate as an oxidant and two anionic surfactants DBSA and SDS at 0 ˚C. From different spectroscopic techniques it can be concluded that there are strong interactions between PpAP/Al_2O_3 and the surfactants. The percentage inhibition efficiency of these polymers obtained from potentiodynamic polarization and EIS measurements are in good agreement, and the corrosion inhibition efficiencies are in the order PpAP/Al_2O_3-DBSA > PpAP/Al_2O_3-SDS. Polarization curves demonstrated that the examined composites behave as a mixed type of inhibitors. In these composites, the uniform increasing inhibition efficiency as a function of the concentration deals with the adsorption phenomenon; the adsorption of inhibitors on the surface of MS is indicated by decrease in the double layer capacitance. The inhibition is due to the adsorption of the inhibitors on the steel surface and results in blocking the active sites. Adsorption follows Langmuir adsorption isotherm.

References

1. Trabanelli G. Corrosion 1991;47:410-419.
2. Jeyaprabha C, Sathiyanarayanan S, Venkatachari G. J Appl Polym Sci. 2006;101:2144-2153.
3. Abdallah M. Corros Sci. 2002;44:717-728.
4. Singh AK, Quraishi MA. Corros Sci.2010;52:1529-1535.
5. Singh AK, Quraishi MA. Corros Sci. 2010;52:1373-1385.
6. Hosseini M, Mertens SFL, Ghorbani M, et al. Mater Chem Phys. 2003;78:800-808.
7. Hur E, Bereket G, Duran B, et al. Prog Org Coat. 2007;60:153-160.
8. El Azhar M, Mernari B, Traisnel M, et al. Corros Sci. 2001;43:2217-2227.
9. Zhao T, Mu G. Corros Sci. 1999;41:1937-1944.
10. Srikanth AP, Sunitha TG, Raman V, et al. Mater Chem Phys. 2007;103:241-247.
11. Yavuz AG, Gok A. Synth Met. 2007;157:235-242.
12. Xu JC, Liu WM, Li HL. Mater Sci Eng C. 2005;25:444-447.
13. Thenmozhi G, Santhi RJ. Int J Sci Resear. 2014;3:378-384.
14. Ehsani A, Mahjani MG, Jafarian M. Synth Met. 2012;162:199-204.
15. Thenmozhi G, Mohanraj G, Madhusudhana G, et al. J Polym. 2014;ID827043.
16. Zheng J, Li G, Ma X, et al. Sens Actuators B: Chem. 2008;133:374-380.
17. Bian C, Yu Y, Xue G. J Appl Polym Sci. 2007;104:21-26.
18. Li J, Zhu L, Wu Y, et al. Polymer. 2006;47:7361-7367.
19. Thenmozhi G, Arockiasamy P, Santhi RJ. Int J Electrochem. 2014; ID961617.
20. Saliyan VR, Adhikari AV. Corros Sci. 2008;50:55-61.
21. Arockiasamy P, Sheela XQR, Thenmozhi G, et al. Int J Corros. 2014; ID679192.
22. Tang Y, Yang X, Yang W, et al. Corros Sci. 2010;52:1801-1808.
23. Bentiss F, Traisnel M, Lagrenee M. Corros Sci. 2000;42:127-146.
24. Aridoss G, Kim MS, Son SM, et al. Adv Polym Tech. 2010;21:881-887.
25. Quraishi MA, Rawat J, Ajmal M. J Appl Electrochem. 2000;30:745-751.
26. Bayol E, Kayakirilmaz K, Erbil M. Mater Chem Phys. 2007;104:74-82.